Y.-H. Truei, T. Gu, G.-J. Tsai, and G. T. Tsao, "Large-Scale Gradient Elution Chromatography," in Advances in Biochemical Engineering/Biotechnology, Vol. 47, 1-44, Springer-Verlag, Berlin-New York (1992).

Large-Scale Gradient Elution Chromatography

Yung-Huoy Truei, Tingyue Gu, Gow-Jen Tsai and George T. Tsao
School of Chemical Engineering, and Laboratory of Renewable Resources Engineering, A. A. Potter Engineering Center, Purdue University, West Lafayette, IN, USA

The goal of this chapter is to provide practical strategies for large scale separations by gradient elution chromatography. A detailed model has been developed for gradient elution systems considering interference effect, longitudinal diffusion, film mass transfer, intraparticle diffusion, mixing mechanism of the mobile phases, Langmuir-type adsorption and desorption kinetics. This detailed model can be solved by an efficient and robust numerical procedure. Hence, the optimizaton strategy of gradient elution has been developed through the calculation using this detailed model. This detailed model can precisely predict the band position, profile and width at various gradient concentrations, gradient periods, flowrates, and column lengths, in fair agreement with the experimental results. As a result of optimization, an optimal column length may exist. All the input parameters in this model have been either experimentally measured or estimated through empirical correlations. An alternative instrument for large-scale production using gradient elution has been suggested compared with conventional gradient elution instrument. The tolerance of the gradient elution processes to the fluctuation of input parameters has also been discussed.

Advances in Biochemical Engineering
Biotechnology, Vol. 47
Managing Editor: A. Fiechter

List of Symbols

Symbol	Description
a	constant in Langmuir adsorption equation (−)
A	mobile phase component which has stronger affinity with the stationary phase
b	constant in Langmuir adsorption equation $(M)^{-1}$
B	mobile phase component which has weak affinity with the stationary phase
C	concentration (M)
C_b	eluate concentration (M)
CHY-A	a-chymotrypsinogen A
C_m	eluent concentration (M)
CYT-C	cytochrome C
d	molecular diameter (cm)
dp	pore diameter (cm)
D	Brownian diffusivity ($cm^2\ s^{-1}$)
D_b	axial dispersion coefficient ($cm^2\ s^{-1}$)
D_p	intraparticle diffusivity ($cm^2\ s^{-1}$)
F	flowrate ($ml\ s^{-1}$)
k	film mass transfer coefficient ($cm\ s^{-1}$)
k′	capacity factor (−)
L	column length (cm)
LYS	lysozyme
Mr	molecular weight (−)
Pe_L	Peclet number of axial dispersion, vLD_b^{-1} (−)
Re	Reynolds number, $2R_p\varepsilon_b v\rho\eta^{-1}$ (−)
RIB-A	ribonuclease A
R_p	particle radius (cm)
Sc	Schmidt number, $\eta r^{-1}D^{-1}$ (−)
t	time (s)
t_R	retention time (s)
t_W	band width (s)
v	interstitial velocity ($cm\ s^{-1}$)
V	liquid volume (ml)
V_m	internal volume of the mixer (ml)
V_s	specific volume ($ml\ g^{-1}$)
z	ZL^{-1} (−)
Z	axial coordinate (cm)
Z′	proportional coefficient (−)

Greek Letters

α	constant coefficient (−)
β	constant coefficient (−)
δ	standard deviation of the Gaussian band (−)
ε_b	bed void fraction (−)
ε_p	particle porosity (−)
η	viscosity of the mobile phase ($g\ cm^{-1}\ s^{-1}$)
γ	constant coefficient (−)
λ	dd_p^{-1} (−)
ρ	density of the mobile phase ($g\ ml^{-1}$)
τ	tvL^{-1} (−)
τ_{imp}	dimensionless time duration of the sample injection (−)

Subscripts

i	ith component
0	initial value

1 Introduction

This chapter is not intended to be a conventional review of gradient elution chromatography. Instead, the goal of this chapter is to provide practical strategies for large-scale separations using this method. Comprehensive reviews have provided its fundamentals and applications [1–4] for analytical purposes. In response to the increasing need for high purity bioproducts, advances in analytical liquid chromatography are being exploited for bioseparations [5]. Many of these bioproducts are proteins or other macro-molecules. However, most current theories and application strategies in gradient elution chromatography were developed for analytical purposes of small compounds, and they might not be appropriate for large-scale separations of macro-molecules, which will be generally described in this section and in detail in the remaining sections of this chapter.

Analyses are usually handled with small sample sizes and with dilute sample concentrations in the linear range of isotherms, with which the retention time and the band profiles of eluates are independent of the composition of the sample. By the same token, the elution bands in chemical analysis are usually treated as symmetrical Gaussian bands, whose band widths are always equal to 4δ, where δ is the standard deviation of the Gaussian band [4]. Under the assumption of Gaussian elution bands, it is a common belief that an increase in column length always improves separation performance. However, large-scale separations must be run with large sample sizes and/or with elevated sample concentrations, which have been shown to result in significant tailing of the bands with the concomitant loss of separation efficiency [6]. Thus, the nonlinearity of isotherms are often utilized in large-scale separations, in which the retention time and the band profiles of eluates, which are often asymmetrical, are dependent on the composition of the sample, which is called the interference effect [7]. For such asymmetrical elution bands of significant tailing, the common belief that an increase in column length always improves separation performance must be reexamined for large-scale separations. In an industrial scale operation, the greater length may mean an increased dispersion and thus affects the performance adversely. An effort to determine an "optimal" column length may be needed for large-scale separations.

The majority of current gradient elution theories emphasize the features regarding the chemical interaction between the stationary phase and the mobile phase [8–11]. Transport and kinetic problems in gradient elution systems are often overlooked, but can be significant in large-scale separations, especially for macro-molecules [12, 13]. Without considering the transport and kinetic effects, the band broadening and the band separation are difficult to elucidate [14]. Recently, the knowledge gained through studies in other fields of chemical engineering has been extended into the field of chromatographic separations. There is a large body of literature on band broadening due to the effects of transport and kinetics [15–22]. However, it is a challenge to develop a practical and realistic optimization strategy for large-scale separations by gradient elution chromatography considering the transport and the kinetic effects.

Consideration of the transport and the kinetic mechanisms makes the mathematical modeling very complex. Analytical solutions are usually unavailable for such a complex model [23]. As a result most scale-up processes of gradient elution chromatography have been carried out empirically [24]. The plate theory [25–27] and the lumped method [28, 29] have long been used to simplify the mathematical model. On the other hand, the simplifications which do allow analytical solutions often fail to reflect the reality of the system. For instance, the plate theory is limited to symmetrical Gaussian bands, and the lumped method is incapable of predicting the dynamic dependence of the chromatographic behavior on the input parameters, such as the flowrate, the particle size and the column length. Therefore, a detailed mathematical model considering the interference effect, the transport and the kinetic mechanisms must be used in predicting optimization of large-scale gradient elution chromatography. Recently, an efficient and robust numerical procedure has been developed for the solution of the complex mathematical model [30]. In addition, band broadening phenomena may be caused by different mechanisms including transport, kinetics, thermodynamics and in-column reactions, and these are often difficult to distinguish from one another [31, 32]. In other words, a detailed model with many adjustable parameters is usually able to fit most of the band profiles. Hence, the controlling mechanism must be determined before the detailed model is used. Otherwise, any further extrapolation and conclusions drawn from such a complex model without validating the controlling mechanism may be unrealistic.

The existing gradient elution instrumentation and procedures were also developed for analytic purposes. The simple extension of analytical instrumentation and procedures may not be sufficient for large-scale separations. For instance, when two or more mobile phases are mixed in gradient elution chromatography, air bubbles are often formed and then captured in the closed mixer, which may lead to distortion of gradient shape [33]. In the laboratory, various methods, including heating, helium and nitrogen gas purging, decompression, ultrasonification and using special degassing devices, are employed for removal of air from the mobile phases. These degassing methods are impractical in large-scale separations. An alternative instrument of gradient elution chromatography must be developed for industrial separations to prevent problems with air bubbles. Furthermore, the proportioning of mobile phases in gradient elution chromatography must be precisely controlled, otherwise the gradient shape may be distorted [1, 2, 4]. However, a variety of other causes can also lead to the distortion of the gradient shape [1, 2, 4]. These causes include the inaccurate flowrate of the pump, poor mixing of the mobile phases, and large hold-up volume of the mixer, as well as a large volume between the mixer and the column inlet. As a consequence, there is no question that highly precise and accurate gradient shapes are difficult to reproduce, particularly on various gradient devices [4, 34]. The distortion of gradient shape can be more serious in

large-scale separations because industrial operations are usually not easily controlled as precisely as laboratory analyses. Therefore, the distortion of gradient shape must be solved in large-scale separations.

The retention relationship of the eluate concentrations and the eluent concentration describes how the eluent affects the retention of the eluates following the continual increase of the elution strength throughout the gradient period. Many conventional retention relationships developed for small molecules, such as the mass action law for small ions in ion exchange chromatography [35], have been extended to proteins. However, recent studies show the adsorption mechanism of proteins in ion exchange chromatography is not solely ion exchange [36–38]. One example is the significant hydrophobic interaction of macro-molecules in ion exchange chromatography, which has not been an important consideration for small compounds [39, 40]. Hence, Regnier has called the stoichiometric model as a non-mechanistic model and used the term electrochemical interaction chromatography (EIC) instead of ion exchange chromatography (IEC) for the adsorption of proteins in ion exchange systems [36]. Several empirical retention relationships of proteins have been developed [36, 39, 41].

The chromatographic procedures can be more precisely controlled in the laboratory than in an industrial setting. Therefore, the consistency of the gradient shape may not be easily achieved in industry. Other input parameters of chromatographic separations, such as feed concentrations, eluent concentration and pH value, can also vary from batch to batch in industrial operations. The tolerance of separation processes to the fluctuation of input parameters must also be considered in large-scale separations of gradient elution chromatography.

2 General Description

2.1 Overview

Gradient elution chromatography is a powerful tool for chemical analysis due to its broad range of retentivity, high peak capacity and short operation cycle [42]. The advantages of gradient elution chromatography are achieved by increasing elution strength during the gradient period, in contrast to the unchanged elution strength in isocratic elution chromatography. The continual increase of elution strength throughout the gradient period, known as a solvent gradient, is usually achieved by the proportioning of multiple mobile phases with a gradient former. Temperature gradient, flowrate gradient and column-material gradient or column switch (also called tandem columns) are alternatives to solvent gradient, but will not be discussed in this chapter. In solvent gradient, the gradient former programs the composition change of the mobile-phase mixture. Either the pumps or the valves, which must be programmable, are controlled by the gradient former in order to proportion the mobile phases (detailed in Sect. 3). The commonly used binary gradients are formed by two mobile phases, a weak component, called mobile-phase A in this chapter, and a strong one, called mobile-phase B. However, ternary or more complex gradients are also used particularly with the aim of eliminating the demixing effect of the mobile phases, which is caused by the incompatibility of the mobile phases [1, 4]. A mixer is also needed to mix the mobile phases and can be either a dynamic mixer or a static mixer (detailed in Sect. 3). Furthermore, the change of the mobile-phase composition change with time is called gradient shape. Gradient shape can be simply classified as continuous gradient and stepwise gradient, shown in Fig. 1. The continuous gradient includes linear gradient, also known as linear solvent strength (LSS) gradient [4] (see Figs. 4a and 4b), and nonlinear gradient (see Fig. 5). The stepwise gradient is composed of multiple steps of isocratic elution. Displacement chromatography, which uses a step-up of the displacer solution to displace the pre-loaded sample compounds, can be classified as a stepwise gradient chromatography. However, a complex gradient, such as multi-stepwise linear gradient (also known as segmented linear gradient) [43] (see Fig. 6), can be composed of the various simple gradients as well as isocratic steps. Usually, the eluent concentration increases during the continuous gradient period; while it decreases in hydrophobic interaction chromatography [40] (see Fig. 4b). In this chapter, only the linear gradient and the stepwise gradient will be discussed and compared due to the inconvenient complexity of other gradient techniques. Before the gradient starts, the column is equilibrated with the starting mobile-phase. After the end of a previous gradient run, the column must be completely reequilibrated with its initial mobile-phase before the next injection, usually by switching to its initial mobile phase rather than by a reverse gradient [1]. Incomplete equilibrium with the initial mobile phase after the prior run will

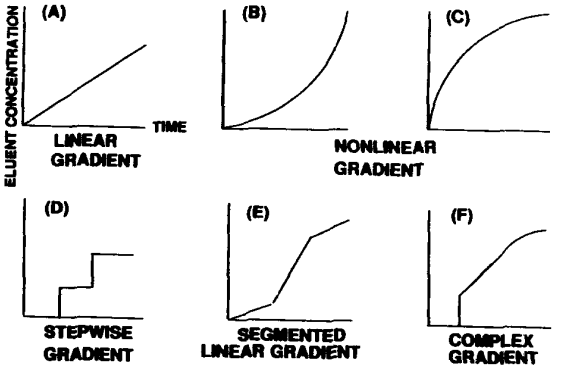

Fig. 1. Classification of gradient shapes

cause earlier elution and poor separation of the sample compounds in the next run. The sample compounds are usually dissolved in the initial mobile phase.

2.2 *Advantages*

In isocratic elution chromatography, the strongly retained sample compounds tend to tail and have late retention, shown in Fig. 2. To make these late-eluting bands sharper and elute faster with stronger elution strength, the weakly retained eluates might be poorly separated, shown in Fig. 3. However, in

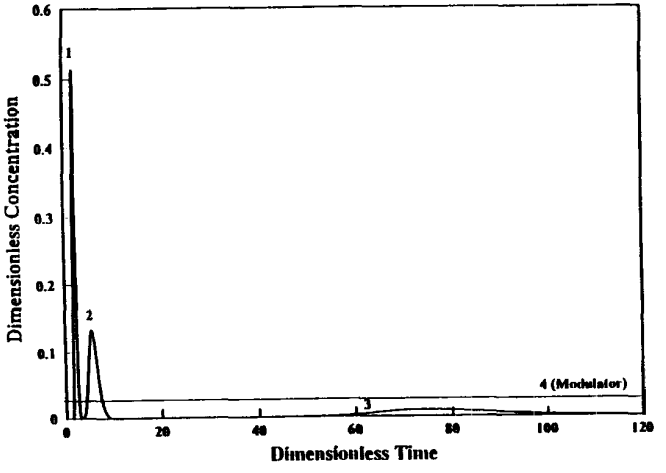

Fig. 2. Isocratic elution chromatogram calculated through the detailed model in the hydrophilic range of the retention relationship

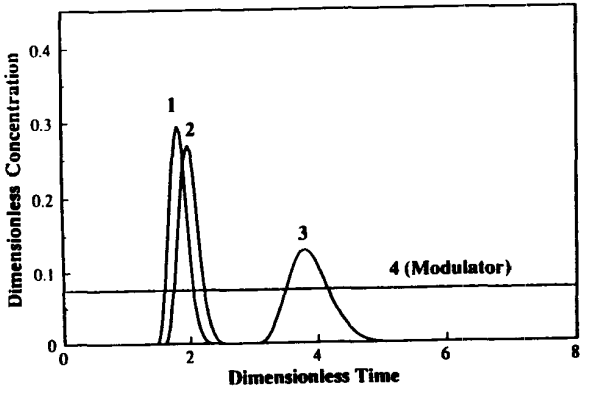

Fig. 3. Isocratic elution chromatogram at higher eluent concentration than in Fig. 2 calculated through the detailed model in the hydrophilic range of the retention relationship

gradient elution chromatography, the strongly retained eluates can be effectively stripped from the column by the continual increase of elution strength throughout the gradient, after the weakly retained eluates are well separated, as shown in Fig. 4. For this reason, the resulting bands are sharp, which means large peak capacity, and the separation cycle is short. Thus, gradient elution has great advantages versus isocratic elution in separating sample compounds which differ widely in retention on a chromatographic column, which is very common

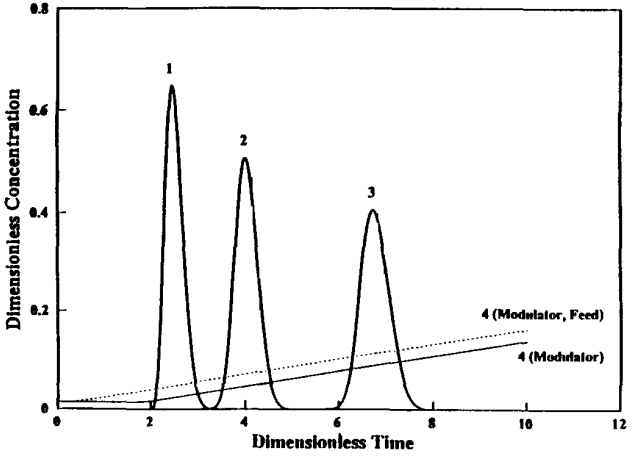

Fig. 4a. Linear gradient elution chromatogram calculated through the detailed model in the hydrophilic range of the retention relationship

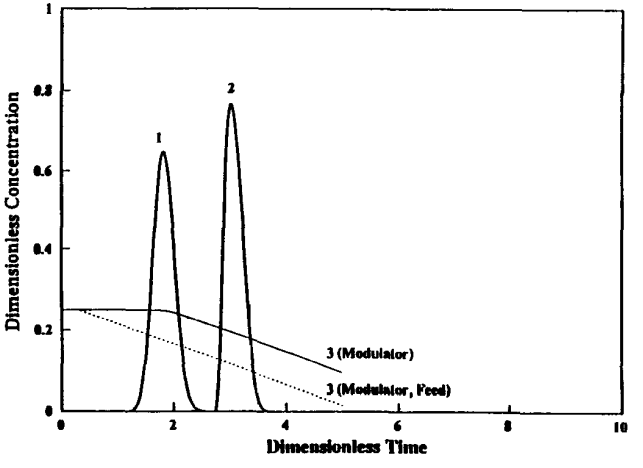

Fig. 4b. Linear gradient elution chromatogram calculated through the detailed model in the hydrophobic range of the retention relationship

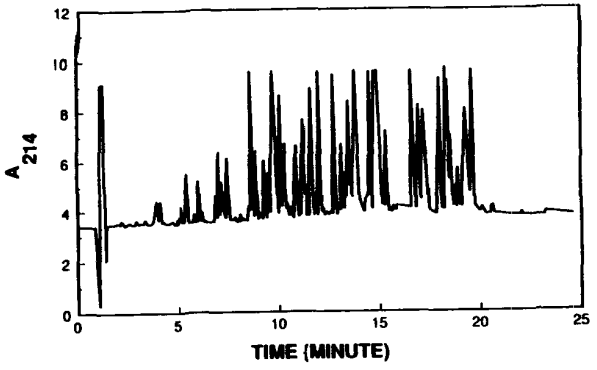

Fig. 5. Tryptic map of r-tissue plasminogen activator. 25 min linear gradient from 0 to 100% mobile phase (B); mobile phase (A): water/TFA, pH = 3, (B): acetonitrile: water = 60:40/TFA, pH = 3; column: Supelco RPC, LC18DB; detection: UV at 214 nm

in separations. Moreover, the gradient devices have been automated and commercially available. As a result, gradient elution chromatography has become a popular analytical technique in the laboratory. A case in point is the tryptic mapping of r-tissue plasminogen activator using gradient elution chromatography. Numerous peaks can be obtained in a single tryptic mapping chromatogram, shown in Fig. 5. Consequently, gradient elution chromatography provides fast and highly resolved separations, which also implies high loading capacity.

2.3 *Disadvantages*

Gradient elution chromatography is not a simple technique. The difficulties of reproducing the results, optimizing the conditions as well as scaling-up gradient elution separations are well known [34]. These difficulties occur because of both the theoretical and practical limitation of gradient elution. The theoretical calculation of gradient elution was limited by lack of the analytical solutions to the detailed model of gradient elution systems, that consider interference, transport and kinetic effects. Hence, further simplification is necessary in order to derive analytical solutions. The major simplifications include the assumption of Gaussian elution bands, linear chromatographic behavior with small sample sizes and dilute sample concentrations, simple retention relationships, and neglect of the transport and kinetic effects for the comparison of the existing models on gradient elution chromatography. However, as mentioned in Sect. 1, these simplifications have not been validated for large-scale separations, particularly of proteins. Several workers considered the transport or kinetic effect, but used lumping techniques to simplify the model and obtain analytical solutions, and ignored the interference effect [28, 29]. Likewise in gradient elution, isocratic elution also has the same theoretical limitation. However, it is much more difficult to calculate effluent profiles for gradient elution than for isocratic elution due to the complication of line-dependent mobile phase

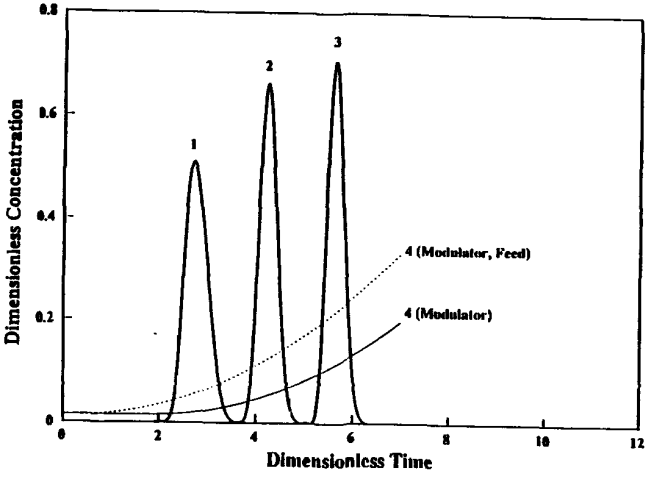

Fig. 6. Nonlinear gradient elution chromatogram calculated through the detailed model in the hydrophilic range of the retention relationship

composition. Numerical methods are currently the only solutions to the detailed model of the gradient elution system. However, an efficient and robust numerical procedure must be developed for such a detailed model, otherwise, the computational time will be expensive [30]. As a consequence, most scale-up processes of gradient elution chromatography have been carried out empirically [24].

The practical limitation of gradient elution chromatography is attributed to instrumental errors of the gradient devices. The basic requirements of gradient instrumentation is that they ensure consistency between the programmed gradient shape and the resulting gradient shape as it enters the inlet of the column. They require accurate and precise proportioning of mobile phases during the gradient run, and good mixing of the mobile phase mixture before it reaches the column [4]. However, in practice, a variety of causes for instrumental errors lead to distortion of the gradient shape. These include air bubbles, incomplete mixing of mobile phases, hold-up volume of the mixer and inaccurate flowrate of the pumps or valves over certain ranges of the gradient [44]. As previously mentioned, the air bubbles are often formed and captured by the closed mixer during the mixing of mobile phases [33]. Complete degassing of mobile phases by heating, helium and nitrogen gas purging, decompression, ultrasonification or the use of special degassing devices, is necessary to prevent air bubbles. The widely used reciprocating pumps need an additional pulse damper, and have limited accuracy in the 0–10% and 90–100% ranges of the gradient [4]. The larger the hold-up volume of the mixer, the more even is the mobile-phase mixture leaving the mixer [1, 4]. The hold-up volume between the mixer and the inlet of the column can also distort the gradient shape [4]. In addition, baseline shift or instability is another general problem in gradient elution, especially

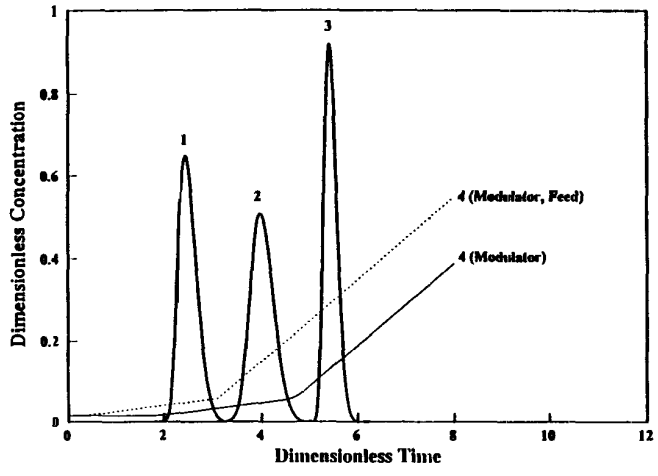

Fig. 7. Segmented linear gradient elution chromatogram calculated through the detailed model in the hydrophilic range of the retention relationship

when the mobile phases are incompatible. This problem will not distort the gradient shape, but will lead to the difficulty in quantifying the elution bands. The causes for baseline shift are complicated [45]. These instrumental errors result in difficulty in reproducing the gradient results, particularly on different gradient devices. These practical problems can be more serious in large-scale separations of gradient elution due to the rough conditions of industrial operations. The major goal of this chapter is to provide practical strategies to solve both the theoretical and the practical problems of gradient elution for large-scale separations. The results of gradient elution must be reproducible for repetitive industrial processes.

3 Equipment

3.1 Analytical Devices

The reproducibility of gradient elution results depends greatly on the performance of the instrumentation, as mentioned earlier. However, it is not easy to control precisely the composition of the mobile phase in gradient elution. In this context, several instrumental designs for gradient formation have been utilized [1, 4, 46–48]. Several workers have succeeded in reviewing and comparing the gradient devices [1, 49–51]. Most gradient devices have been commercially available and automated for laboratory analysis. These devices can be simply

classified according to whether the mixing of mobile phases occurs at high pressure (see Fig. 8 for the major device of this type) or at low pressure (see Fig. 9 for the major device of this type). For high pressure mixing, the mixer is located downstream of the pumps and must be mechanically strong enough to undergo the high pressure generated by the pumps; while for low pressure mixing, the mixer is located upstream of the pump and consequently, mechanical strength requirements are less stringent. Furthermore, each mobile phase needs an individual pump for high pressure mixing, and only one pump is needed for low pressure mixing. For high pressure mixing, the proportioning of the mobile phases is carried out by controlling the flowrate of each pump, which must be programmable. Likewise, for low pressure mixing, programmable valves are used to perform the proportioning of the mobile phases. For both high and low pressure mixing, a controller, called the gradient former, is always needed to carry out the proportioning of mobile phases through pumps or valves. However, for a stepwise gradient, a single unprogrammable pump is sufficient, and the gradient former and the mixer are not necessary, although a flow-path switch is needed for changing the mobile phases. Four input parameters, which are gradient period, total flowrate, initial and final mobile-phase compositions, are usually fed into the gradient former for a linear gradient run. For a stepwise gradient run, the time and the mobile-phase composition of each step are the input parameters of the gradient former. Either a dynamic or a static mixer is also used for the mixing of the mobile phases. Both mixers are of the closed type. The dynamic mixer possesses active mechanical agitation, while

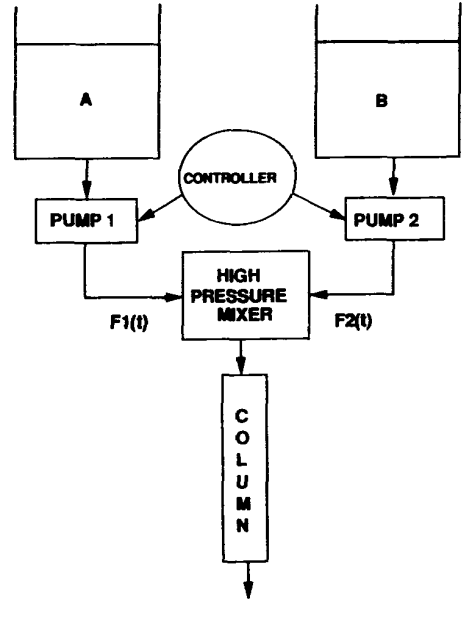

Fig. 8. High-pressure mixing gradient elution chromatographic instrumentation

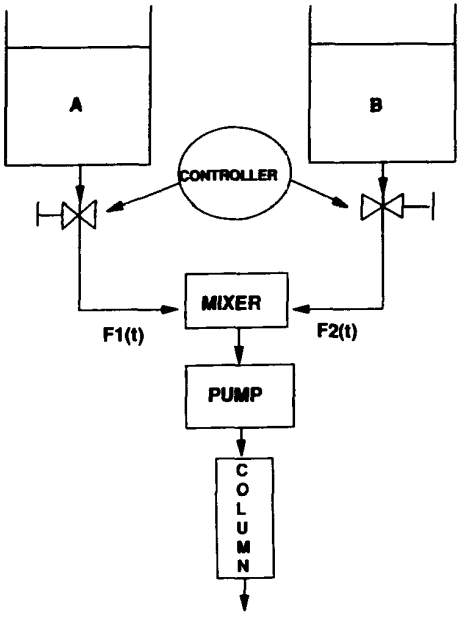

Fig. 9. Low-pressure mixing gradient elution chromatographic instrumentation

the static mixer does not. In principle, a T-connection can be used as a static mixer. However, a big hold-up volume of the static mixer is usually needed to dampen the turbulence arising from the mixing of the mobile phases. Figures 10 and 11 show how the turbulence can be built up and eventually distorts the programmed gradient shape due to the incompatibility of the mobile phases that results when a T-connection is used as a static mixer. In this case, the more

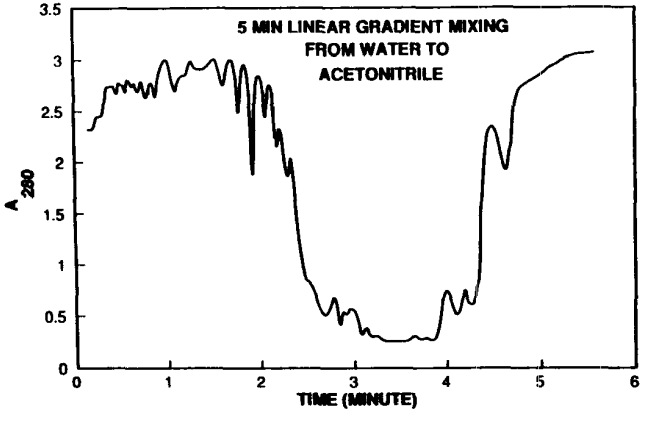

Fig. 10. Resulting gradient shape of 5 min linear gradient elution from water to acetonitrile with a T-connector as a static mixer at the flowrate of 1 ml min^{-1}

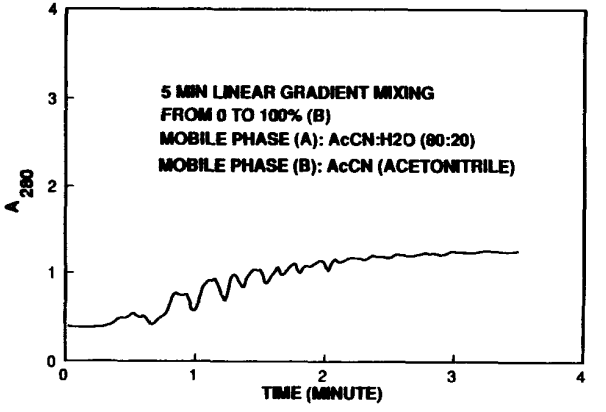

Fig. 11. Resulting gradient shape of 5 min linear gradient elution from a mixture of acetonitrile and water (80:20) to acetonitrile with a T-connector as a static mixer at the flowrate of 1 ml min^{-1}

incompatible the mobile phases are, the more turbulence can be generated. However, the hold-up volume of the mixer also can distort the programmed gradient shape [1, 4]. The larger the hold-up volume of the mixer, the more uniform is the mobile-phase mixture leaving the mixer [4], shown in Fig. 12. Figure 13 shows that for long gradient periods, the resulting gradient shape seems the same as the programmed except for a delay time, which is approximately equivalent to the average residence time of the mixer. But, for fast separations or short gradient period, the gradient shape is totally distorted by the hold-up volume of the mixer, as also shown in Fig. 13. The extent of the distortion of the gradient shape is proportional to the hold-up volume of the

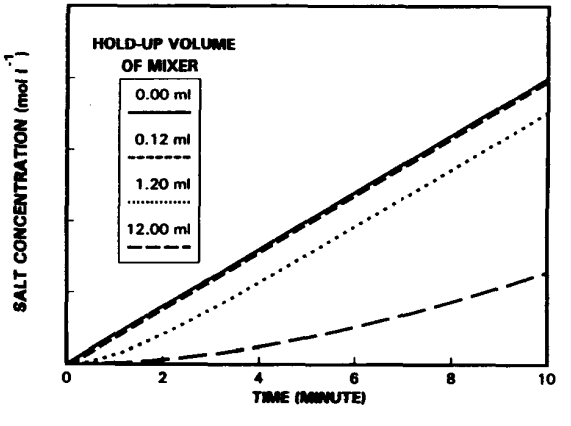

Fig. 12. Distortion of gradient shape by the hold-up volume of mixer in 10 min linear gradient elution from 0 to 2 mol l^{-1} salt at the flowrate of 1 ml min^{-1}

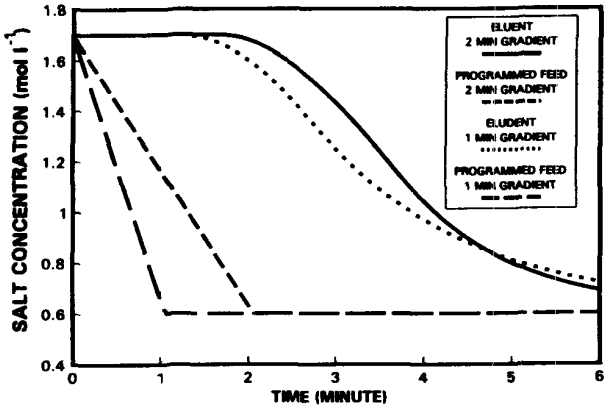

Fig. 13. Distortion of linear gradient shape by the hold-up volume, 1.2 ml, at various gradient periods from 1.7 to 0.6 mol l^{-1} salt at the flowrate of 1 ml min^{-1}

mixer. Hence, the static mixer generally is sufficient only for very compatible mobile phases, and usually gives worst gradient results, even though it is cheaper than the dynamic mixer. As a consequence, a dynamic mixer which can provide perfect mixing with minimal hold-up volume will be the best choice for mixing if the cost consideration is not a problem. The hold-up volume between the mixer and the inlet of the column also can distort the gradient shape [4]. However, mixing mechanisms have been overlooked in the existing models of gradient elution chromatography. We believe that neglect of the mixing mechanism in the gradient system is one of the major reasons for the nonreproducibility of the gradient results and the difficulty in predicting and optimizing the gradient conditions [4, 34]. In addition to the mixing of the mobile phases, the inaccurate flowrate of the pumps also can distort the gradient shape. This problem especially occurs at low flowrate, i.e., in the 0–10% and 90–100% ranges of the gradient using the popular reciprocating pumps, as shown in Figs. 14 and 15 [1, 4]. In principle, Figs. 14 and 15 should be identical if the flowrate is accurate in the 0–10% range of the gradient. In fact, they are different. Thus, these gradient ranges must be avoided or a positive displacement pump should replace the widely used reciprocating pumps.

Apparently, the gradient device of high pressure mixing is more expensive than that of low pressure mixing due to the high-pressure mixer and additional pumps. However, it will usually prove to be worth the additional expense. Mobile phases usually contain some dissolved air from the atmosphere. When the mobile phases are mixed in the mixer, the resulting mixture are often supersaturated with dissolved air which is then released as bubbles. If air bubbles are released in the mixer, they are captured in the closed mixer and then pumped into the gradient system. Many problems including the distortion of the gradient shape arise from the formation of air bubbles. However, when the

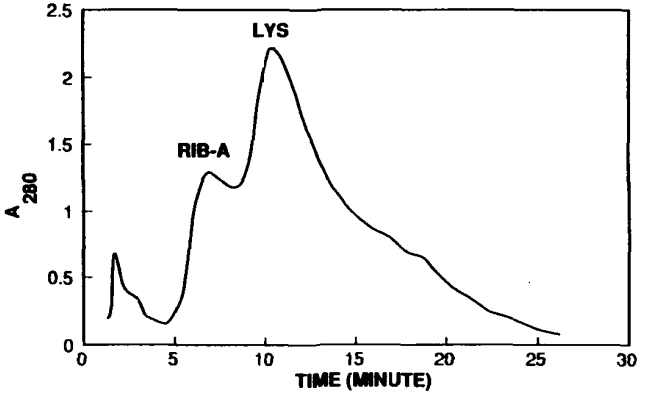

Fig. 14. Chromatogram of 15 min linear gradient elution from 0 to 100% mobile phase (B) on a column of Zorbax Bio-series WCX-300 (80 × 6.2 mm) at the flowrate of 1 ml min^{-1}; mobile phase (A): 10 mmol l^{-1} ammonium sulfate in 20 mmol l^{-1} phosphate buffer solution, pH 6, (B): 100 mmol l^{-1} ammonium sulfate in 20 mmol l^{-1} phosphate buffer solution, pH 6

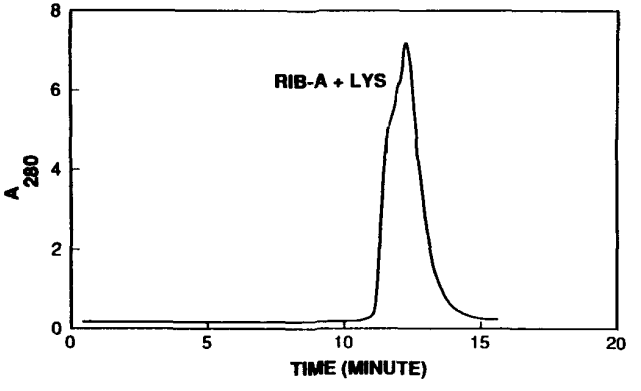

Fig. 15. Chromatogram of 15 min linear gradient elution from 0 to 10% mobile phase (B) on a column of Zorbax Bio-series WCX-300 (80 × 6.2 mm) at the flowrate of 1 ml min^{-1}; mobile phase (A): 10 mmol l^{-1} ammonium sulfate in 20 mmol l^{-1} phosphate buffer solution, pH 6, (B): 1 mol l^{-1} ammonium sulfate in 20 mmol l^{-1} phosphate buffer solution, pH 6

mixing of the mobile phases occurs under high pressure, the solubility of the resulting mixture is higher, and fewer air bubbles might be released. Even though the high pressure mixing cannot completely solve the problems with air bubbles, this problem is usually more severe for low pressure mixing, where extra effort in degassing is normally needed. This implies that the routine costs of gradient runs could be high regardless of the cheap initial instrument cost. The problem with air bubbles is particularly serious in reversed-phase chromatography because the mobile phases generally dissolve air to a widely

different extent. Air bubbles can be formed not only in the mixer but also everywhere down stream of it. According to Bernoulli's equation [52], when the mobile phase passes from a wide cross-section through a narrow section, the increase in the velocity of the mobile phase will result in the decrease of the static pressure and the solubility of air. Then, air bubbles would be released due to the decrease of the air solubility. Therefore, the connector, especially when it is located in between the mixer and the inlet of the column, must have an internal cross-section area as uniform as possible. Complete degassing of mobile phases by heating, helium and nitrogen gas purging, decompression, ultrasonification or using special degassing devices, is necessary. Helium is widely used for degassing due to its low solubility in most liquids compared with air, and its use is treated as a routine operation cost. However, extensive degassing may vaporize the volatile mobile-phase components and change the mobile-phase composition. For instance, in reversed-phase chromatography, the composition of organic solvent and trifluoracetic acid in an aqueous solution can be lower than expected after extensive degassing.

3.2 Large-Scale Separation Devices

Apparently, the existing gradient instrumentation for analytical purposes still has many problems with instrument error. The major problem is that the resulting gradient shape departs from that programmed. This problem can be more serious in large-scale separations due to the more controlled conditions required in industrial operations, if the analytical instrumentation and procedures are simply extended to large-scale separations. Moreover, the conventional ways of degassing in laboratory analysis are impractical in industrial operations. In industry, the gradient shape must be consistent for repetitive industrial separation processes, and the formation of air bubbles must be prevented. Therefore, an alternative design of gradient instrumentation must be developed for industrial operations.

An alternative gradient system reported by Scott [53], shown in Fig. 16, has great advantages in industrial separations, but in contrast has some disadvantages in chemical analysis. This gradient system was reported before the currently strong interest in preparative chromatography, and has not been widely adopted. The Bio-Rad Model 385 gradient former used this idea of instrumentation except the use of gels for gradient formation [54]. This gradient system for high-performance columns is similar to a widely used gradient system for low-performance columns, shown in Fig. 17.

For linear gradient, $F_B = F_A \times 0.5$ (see Fig. 16), and

$$C_A = C_{A0} + (C_B - C_{A0})F_A t(2V_{A0})^{-1} \quad (1)$$

where C denotes the concentration, F the flowrate, t time, V the liquid volume in the vessel, and subscripts A, B and 0 denote vessel A, vessel B and the initial value, respectively. From this equation, it follows that the initial and the final

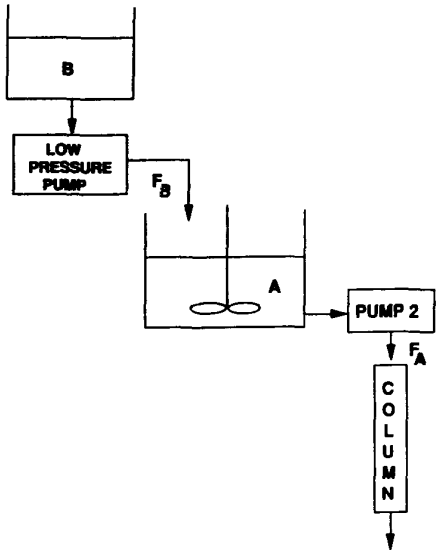

Fig. 16. Gradient elution chromatographic instrumentation of Scott [53]

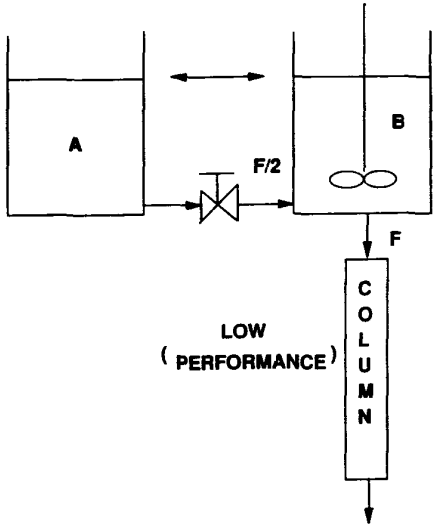

Fig. 17. Low-performance gradient elution chromatographic instrumentation

concentrations of gradient are C_{A0} and C_B, respectively, and the gradient period is $(2V_{A0}F_A^{-1})$.

Its advantages in large-scale separations are:

- Mixing of mobile phases is carried out in an open vessel, which does not capture air bubbles. Hence, extensive degassing is not necessary.

- The mixing of mobile phases occurs in a vessel which originally contains mobile phase A. An additional mixer, especially one with high mechanical strength, is not needed.
- If the mixing in vessel A is efficient, the gradient shape will not be distorted by the hold-up volume of vessel A.
- The flowrates from two vessels remain unchanged. The proportioning controller and programmable valves are not needed. The pumps do not need to be programmable. There will be no problems with inaccurate flowrate in the 0–10% and 90–100% ranges of the gradient.
- The pump between two vessels does not need to be a high pressure pump. A multi-channel pump instead of two pumps can be used for this gradient system, shown in Fig. 18.

Since $F_B = F_A \times 0.5$ for a linear gradient, vessel A needs to be refilled after every gradient run. It is inconvenient for chemical analysis but does not pose a problem for standard industrial procedure. The gradient period needs to be calculated from V_{A0} and F_A, which is impractical for analysis but is also acceptable for repetitive industrial processes. It has been found experimentally that this gradient system, compared to the conventional gradient systems does not exhibit the distortion of gradient shape due to inaccurate flowrate of the pumps, or incomplete mixing of the mobile phases and hold-up volume of the mixer [55], as shown in Fig. 19. The consistency between the resulting gradient shape and the programmed shape through this gradient system has also been experimentally demonstrated to be good [55] and is shown in Fig. 19. In

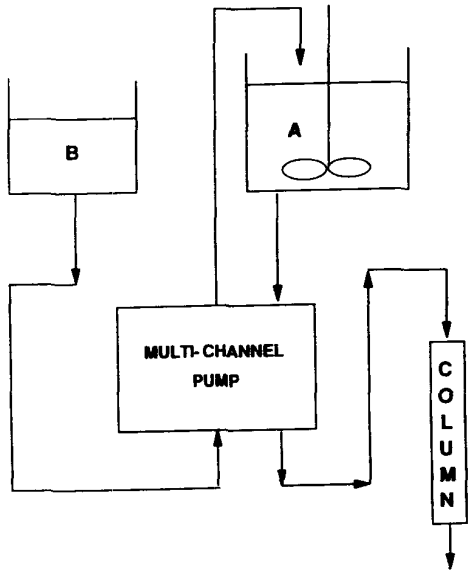

Fig. 18. Gradient elution chromatographic instrumentation of Scott [53] with a multi-channel pump

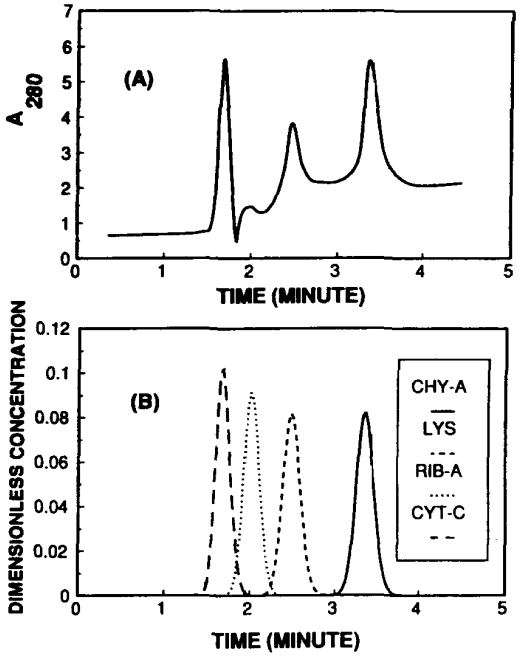

Fig. 19. Chromatograms of 2 min gradient elution from 1.7 to 0.6 mol l^{-1} ammonium sulfate using the gradient elution instrumentation of Scott [53]. (**A**) experimental, (**B**) theoretical through the detailed model; column length: 8 cm; $v = 0.138$ cm s^{-1}

particular, the problem of air bubbles does not arise [55]. Consequently, this gradient system does not pose the practical problems with the instrumental errors which the conventional gradient systems have, is cost effective, and gives reproducible and consistent results. On the other hand, this gradient system is inconvenient for laboratory analysis.

4 Key Mechanisms

4.1 Retention Relationships

There are two major mechanisms which affect the retention of the eluates. The first one is the adsorption isotherm, which describes the relationship between the stationary concentration and the mobile phase concentrations. For multiple components, the multicomponent isotherm also describes the interference effect. The second one is the retention relationship of the eluate concentrations and the eluent concentration, which describes how the eluent affects the retention of the eluates.

Most existing models neglect the interference effect, which is insignificant for chemical analyses due to the small sample sizes and the dilute sample concentrations, but must be considered in preparative and large-scale gradient elution chromatography in which the column is often overloaded in terms of feed size and/or concentration [42]. Thus, the nonlinearity of isotherms is often utilized in large-scale chromatographic separations. This nonlinearity will cause the rear of the band broadened [32], while the leading edge of the bandit steeper. Thus, the band shape is often asymmetric and dependent on the composition of the mobile phase in large-scale chromatographic separations. However, a realistic adsorption equation can precisely elucidate the interference effect and the nonlinear response of the stationary phase on the band shape. The Langmuir adsorption equation is the most widely used for chromatographic separations due to its simplicity and capability of fitting many experimental results of chromatographic adsorption [56]. The extended multicomponent Langmuir adsorption equation is also capable of describing the interference effect [42]. However, the adsorption isotherm must be experimentally measured to validate the adsorption equation.

There are two major mechanisms with which the eluent affects the retentivities of the eluates. The first is the direct competition of the eluent with the eluates directly for binding sites on the stationary phase; here, the eluent is treated as a simple competing reagent. A case in point is the mass action law [35]. The second mechanism is the lowering of the adsorption equilibrium constant of the eluates by the eluent, for example, the ionic strength and the pH value have been used as the elution strength in ion-exchange chromatography [41, 57]. For small molecules, the first mechanism may sufficiently elucidate the elution phenomena in ion exchange chromatography, and a linear relationship between log(k') (k' denotes the capacity factor) and log(Cm) (Cm denotes the eluent concentration) with a positive proportional coefficient β [58–60]. In reversed phase chromatography, Snyder [4] found that another linear relationship between log(k') and Cm would be better. However, such linear relationships are true for proteins only over relatively narrow eluent concentration ranges, and the value of β can be negative [61]. Other types of relationship for k' and Cm have also been developed (see Table 1). Some experimental plots of log(k') vs. Cm or log(Cm) for proteins in ion exchange and reversed phase chromatography have been found to be nonlinear and exhibit minima [36, 37, 62]. Obviously, the role of eluent on the elution of proteins is more complex than a simple competitor [36, 37, 62] (see Fig. 20). Instead, both mechanisms are involved in the retention phenomena of proteins. Hence, an empirical correlation of k' and Cm must be used for proteins in gradient elution chromatography. An empirical correlation of k' and Cm has been developed for both hydrophilic interaction and hydrophobic interaction of proteins in ion exchange chromatographic systems, as follows [39].

$$\log(k') = \alpha - \beta\log(Cm) + \gamma Cm,$$

where α, β and γ are constant coefficients.

Table 1. Comparison of models for gradient elution chromatography

Reference	Correlation* of k' v. C_m	Isotherm	Interaction** type	Gradient method	Axial dispersion	Film mass transfer	Intraparticle diffusion	Kinetic effect
Pitt (60)	(1)	Linear	(1)	Linear	Yes	No	No	Linear
Jandera & Churacek (34, 77)	(1) & (2)	Linear	(2)	Linear	No	No	No	No
Hearn & Grego (62)	(1) & (2)	Linear	(2)	Linear	No	No	No	No
Armstrong & Boehm (78)	(2)	Linear	(2)	Linear	No	No	No	No
Kennedy et al. (79)	(1)	Linear	(1)	Linear	No	No	No	No
Furusaki et al. (24)	(3)	Linear	(2)	Linear	Yes	No	Yes	No
Yamamoto et al. (41)	(3)	Linear	(2)	Linear	No	No	No	No
D'Agostino et al. (80)	(5)	Linear	(2)	Linear	No	No	No	No
Ghrist & Snyder (43)	(2)	Linear	(2)	Linear & Stepwise linear	No	No	No	No
Markowski & Golkiewicz (81)	(1) & (2)	Linear	(2)	Stepwise	No	No	No	No
Martin (82)	(2)	Linear	(2)	Linear	No	No	No	No
Merengo et al. (83)	(6)	Linear	(2)	Linear	No	No	No	No
Antia & Horvath (42)	(1) & (2)	Langmuir (Multicomponent)	(2)	Linear	Yes	No	No	No
Kang & McCoy (84)	(3)	Linear	(2)	Linear	Yes	No	No	No
This Work	(4)	Langmuir (Multicomponent)	(2)	Linear Stepwise linear & Nonlinear	Yes	Yes	Yes	2nd Order

* (1) $\log k' = \alpha - \beta \log C_m$ (2) $\log k' = \alpha - \beta C_m$ (3) $\log (k' - \alpha) \equiv -\beta C_m$
(4) $\log k' = \alpha - \beta \log C_m + \gamma C_m$ (5) $\log k' = \alpha_0 + \alpha_1 C_m + \alpha_2 C_m^2 + \ldots$ (6) $k' = \alpha_0 + \alpha_1 C_m + \alpha_2 C_m^2 + \ldots$

** (1) Modulator competes with eluates for binding sites, but does not affect the k' value of the eluates
(2) Modulator affects the k' values of the eluates, but has negligible adsorption on the stationary phase

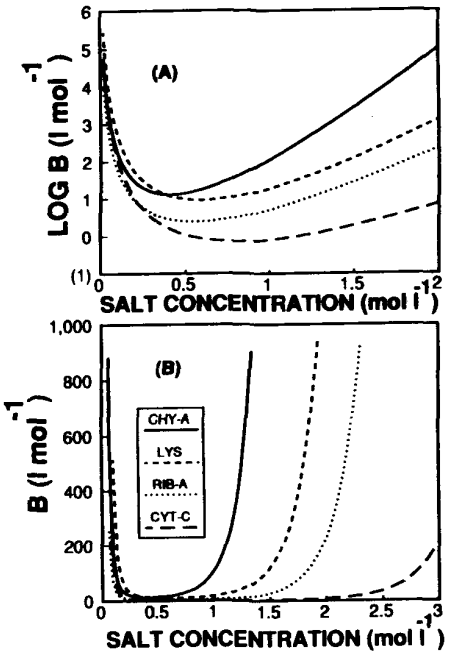

Fig. 20. Retention relationships between b and Cm at pH 6 on a column of Zorbax Bio-series WCX-300 (80 × 6.2 mm)

However, many conventional retention relationships developed for small molecules, such as the mass action law for small ions in ion exchange chromatography, have been inappropriately extended to proteins. First of all, the mass action law cannot account for the hydrophobic interaction of proteins in ion exchange chromatography. Second, the Langmuir adsorption equation is equivalent to the mass action law when the characteristic valence in mass action law is equal to one. But, the characteristic valences of proteins are usually not one [63]. Third, the characteristic valences of proteins vary during the process [63], however, they are assumed as constants in most models which employ the mass action law. Fourth, the mass action law cannot explain slow desorption due to the low possibility of simultaneous dissociation of all of the multiple binding sites of proteins [64].

Four proteins were chosen as the eluates in a recent study of gradient elution chromatography [55]: α-chymotrypsinogen A from bovine pancreas (CHY-A), lysozyme from chicken egg white (LYS), ribonuclease A from bovine pancreas (RIB-A) and cytochrome C from horse heart (CYT-C). Ammonium sulfate was chosen as the eluent. A cation exchange system was chosen for these proteins due to their high pI values. The retention relationships of these proteins and ammonium sulfate [55] were plotted in Fig. 20, which fit the empirical correlation developed by Melander and Horvath [39]. The multicomponent Langmuir

adsorption equation was also used in the study of gradient elution chromatography [55].

4.2 *Mass Transport*

Even though the mixing of mobile phases can distort the gradient shape [4], no current model in gradient elution chromatography considers the mixing mechanism. However, a dynamic mixer can be modeled as a CSTR with an internal volume Vm (ml) [55]. The programmed gradient shape entering the mixer and the resulting gradient shape from this mixer were plotted in Figs. 12 and 13. Figure 12 shows that the distortion of the gradient shape is increased with the hold-up volume of the mixer. For a long gradient period, the resulting gradient shape looks the same as the programmed gradient shape except for a delay time, which is approximately equivalent to the average residence time of the mixer, as shown in Fig. 13. However, for a fast separation or a short gradient period, the gradient shape is totally distorted by the hold-up volume of the mixer, as also shown in Fig. 13. Figure 21 illustrates the deviation of the predicted chromatogram without mixing from that with mixing. Hence, we believe that the neglect of the mixing mechanism in the gradient system is one of the major reasons for the nonreproducibility of the gradient results and the difficulty of predicting the result and optimizing the gradient conditions [55].

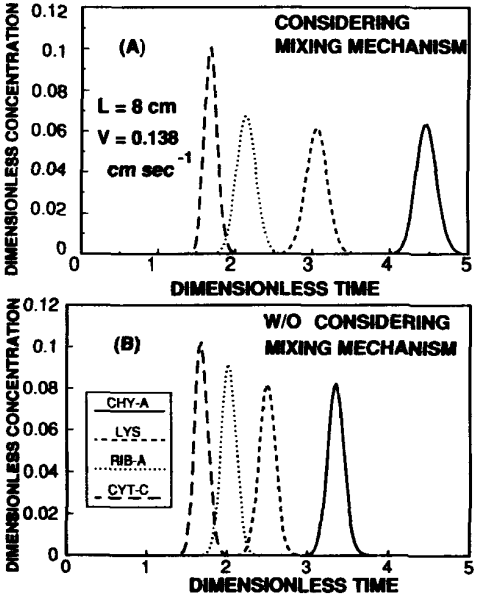

Fig. 21. Comparison of chromatograms of 2 min linear gradient elution from 1.7 to 0.6 mol l^{-1} ammonium sulfate considering the mixing mechanism (A), and without considering the mixing mechanism (B); column length: 8 cm; v = 0.138 cm s^{-1}

Axial dispersion, film mass transfer and intraparticle diffusion are considered as the key mass transfer mechanisms. The eluates are carried by the convective flow of the mobile phase. Along with the convective flow, the injection band can be broadened by axial dispersion. Axial dispersion is caused by Brownian diffusion, eddy diffusion, the boundary layer effect, channeling (if the column was packed improperly), and the wall effect [27]. Then, the eluates need to penetrate through a boundary film on the outer surface of the particles. For most chromatographic particles, the eluates move from the entrance of the pores to the intraparticle surface solely by the intraparticle diffusion. However, for perfusable materials [65], convective flow also occurs within the pores. For macromolecules such as proteins, the hindered diffusion regarding the relative ratio of the molecular size of the eluates to the pore size must be considered for the intraparticle diffusion [66]. The mass transfer coefficient can be estimated by empirical correlations as follows.

The correlation of Chung and Wen [67] can be used to estimate Pe_L, the Peclet number of axial dispersion:

$$Pe_L = (0.2 + 0.11Re^{0.48})L/(2R_p\varepsilon_b) \quad (2)$$

where the Reynolds number $Re = 2R_p\varepsilon_b v\rho\eta^{-1}$, ε_b is the bed void fraction, v is the interstitial velocity (cm s^{-1}), r is the density of the mobile phase (g ml^{-1}), R_p is the particle radius (cm), and η is the viscosity of the mobile phase (g cm^{-1} s^{-1}).

The correlation of Wakao, et al. [68], can be used to estimate k, the film mass transfer coefficient, for the film mass transfer (cm s^{-1}):

$$2R_pkD^{-1} = 2 + 1.45Re^{0.5}Sc^{3^{-1}}, \quad Re < 100 \quad (3)$$

where R_p is the particle radius (cm), D is the Brownian diffusivity (cm^2 s^{-1}), and the Schmidt number $Sc = \eta\rho^{-1}D^{-1}$.

The correlation of Yau et al. [66], is used to estimate D_p, the intraparticle diffusivity, for the intraparticle hindered diffusion:

$$D_p = D(1 - 2.104\lambda + 2.09\lambda^3 - 0.95\lambda^5)2.1^{-1} \quad (4)$$

where $\lambda = d \times d_p^{-1}$, d is the molecular diameter (cm) and d_p is the pore diameter (cm). The parameter d is calculated from the following equation [69]:

$$d = \text{~~2(MrVs×1.246×10}^{-23}\text{)}^{\frac{1}{3}}\text{~~} \; 1.47 \cdot (Mr \cdot V_s)^{1/3} \; (\text{Å}) \quad (5)$$

where Mr is the molecular weight, and Vs is the specific volume (ml g^{-1}).

Recent research [55] has indicated that the distribution of pore size versus intraparticle surface area is broad, as shown in Fig. 22. However, the manufacturers claim the pore size of their products to be narrow, based on the distribution of pore size versus pore volume, shown in Fig. 23. The pore size distribution is important when the hindered diffusion is significant. As long as the macromolecular eluates can penetrate the smaller pores, slow diffusion in these small pores must be a major cause of the broadening of the elution bands regardless of the existence of the larger pores. Therefore, the existence of the small pores must

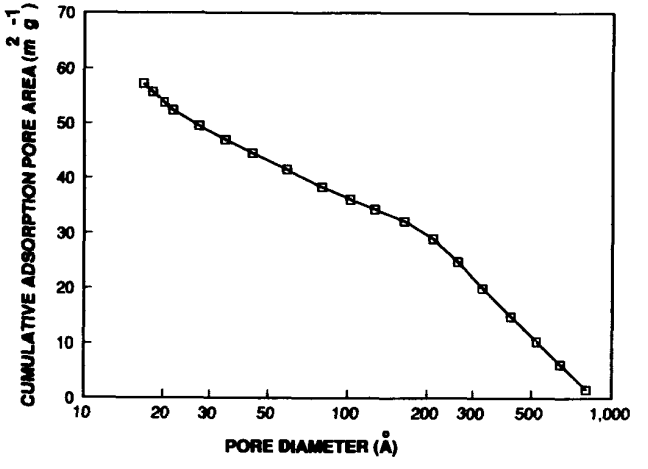

Fig. 22. Distribution of pore size vs. cumulative adsorption pore area of Zorbax Bio-series WCX-300

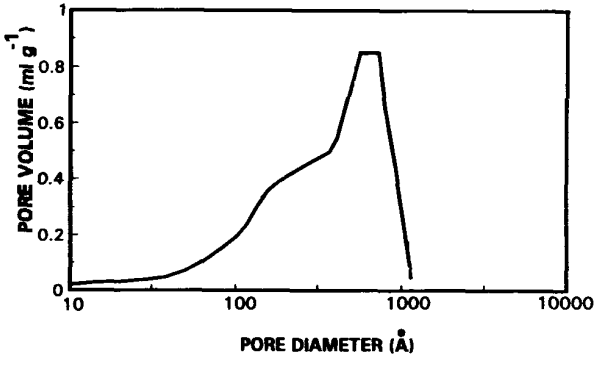

Fig. 23. Distribution of pore size vs. adsorption pore volume of Zorbax Bio-series WCX-300

be avoided for chromatographic materials (including perfusable materials, which contain macro-pores [65]). The pore volume distribution can be precisely measured by the method of nitrogen gas adsorption [70] for the estimation of the intraparticle porosity, ε_p.

4.3 Adsorption and Desorption Kinetics

The adsorption of the eluates is often fast compared with the mass transfer rate, but can be slow enough to broaden the injection band. A case in point is the

affinity chromatography in which the eluates may need numerous collisions before they adsorb on the surface due to specific orientation requirements of the collision [71]. Slow desorption occurs more often than the slow adsorption [71]. Slow desorption can be caused by the multiple binding sites of proteins; it is not easy for the macromolecules to dissociate simultaneously at all binding sites during desorption [64]. Some cases of slow desorption have been discovered in high affinity chromatographic systems [13]. Slow adsorption and desorption can broaden elution bands and reduce separation performance. When the adsorption or the desorption of the eluates is slow, adsorption and desorption kinetics must also be studied in addition to the adsorption equilibrium, and the adsorption and the desorption rate constants also must be experimentally measured. There is no empirical correlation available for the measurement of adsorption and desorption rate constants. Slow adsorption or desorption can be examined easily using frontal technique with a mini- or micro-column at increasing flowrate [55]. When the flowrate is increasing, a minimal breakthrough time results, this is equivalent to the inclusion volume if slow kinetics is the rate limiting step, and is equivalent to the exclusion volume if the mass transfer is the rate limiting step. A mini- or micro-column is used in this experiment to allow for the high pressure drop expected at an elevated flowrate.

5 Optimization

A detailed mathematical model of gradient elution chromatography considering interference effect, longitudinal diffusion, film mass transfer, intraparticle diffusion, mixing mechanism of the mobile phases, Langmuir-type adsorption and desorption kinetics has been developed [30]. It has been applied to simulate large scale gradient elution chromatography. An empirical retention correlation of b and Cm, $\log(b) = \alpha - \beta\log(Cm) + \gamma Cm$, where b is the equilibrium constant in the Langmuir adsorption equation, for proteins in an ion-exchange system was used [39]. The hydrophobic interaction range of eluent concentration is chosen due to the higher relative affinities of the proteins in this range than in the hydrophilic interaction range (see Fig. 20). All the input parameters have been either experimentally measured or estimated through empirical correlations [55]. This model can predict band positions with a relative error of less than 5% at various initial and final eluent concentrations (see Figs. 24 and 25), flowrates (see Figs. 24, 26 and 27), gradient periods (see Figs. 24, and 28–30), and column lengths (see Fig. 31), in linear gradient elution chromatography [55]. Stepwise gradient elution chromatography has also been studied with various stepwise periods and stepwise eluent concentrations (see Figs. 32–36), and compared with linear gradient elution chromatography experimentally and theoretically using the detailed model [55]. However, the required long computation time could be the bottle-neck in using this detailed model. Hence,

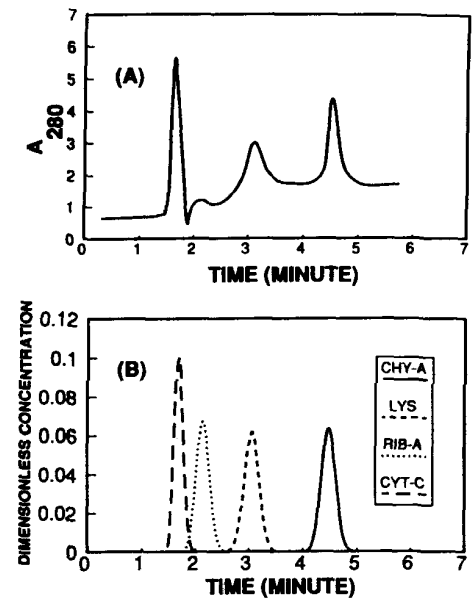

Fig. 24. Chromatograms of 2 min linear gradient elution from 1.7 to 0.6 mol l^{-1} ammonium sulfate. (A) experimental, (B) theoretical through the detailed model; column length: 8 cm; v = 0.138 cm s^{-1}

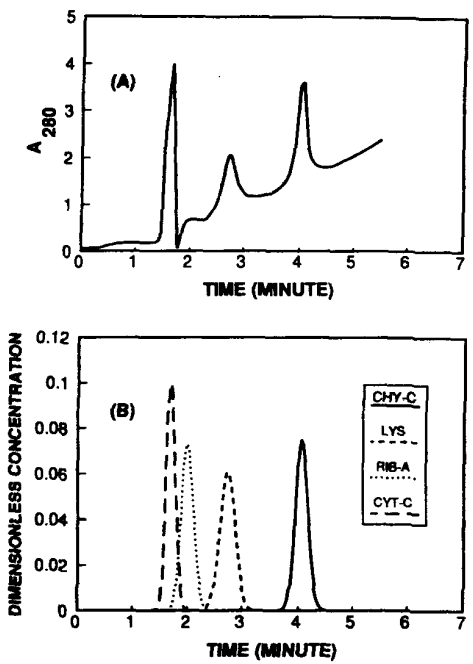

Fig. 25. Chromatograms of 2 min linear gradient elution from 1.6 to 0.4 mol l^{-1} ammonium sulfate. (A) experimental, (B) theoretical through the detailed model; column length: 8 cm; v = 0.138 cm s^{-1}

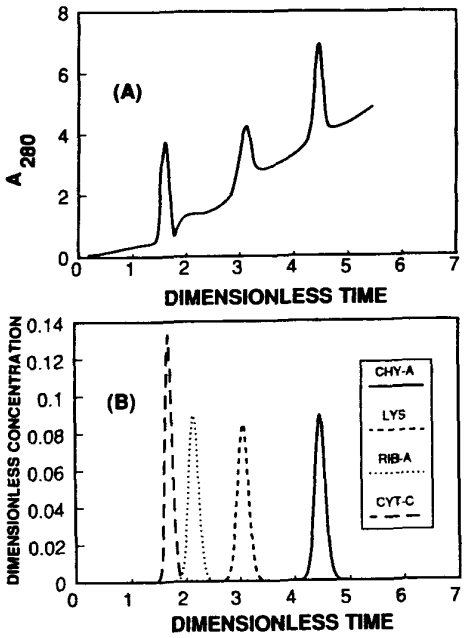

Fig. 26. Chromatograms of 4 min linear gradient elution from 1.7 to 0.6 mol l^{-1} ammonium sulfate. (A) experimental, (B) theoretical through the detailed model; column length: 8 cm; v = 0.069 cm s^{-1}

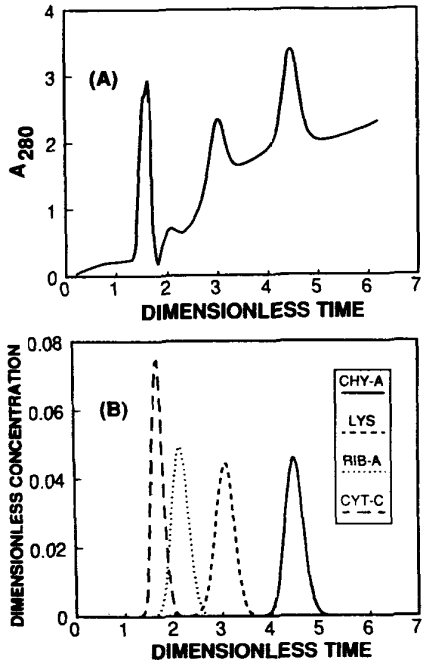

Fig. 27. Chromatograms of 1 min linear gradient elution from 1.7 to 0.6 mol l^{-1} ammonium sulfate. (A) experimental, (B) theoretical through the detailed model; column length: 8 cm; v = 0.276 cm s^{-1}

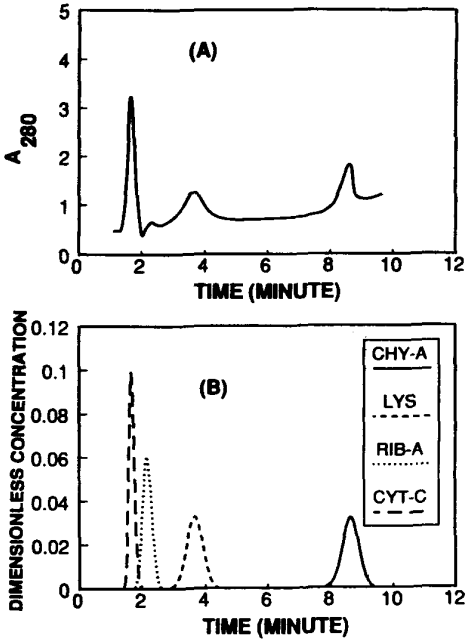

Fig. 28. Chromatograms of 10 min linear gradient elution from 1.7 to 0.6 mol l^{-1} ammonium sulfate. (A) experimental, (B) theoretical through the detailed model; column length: 8 cm; v = 0.138 cm s^{-1}

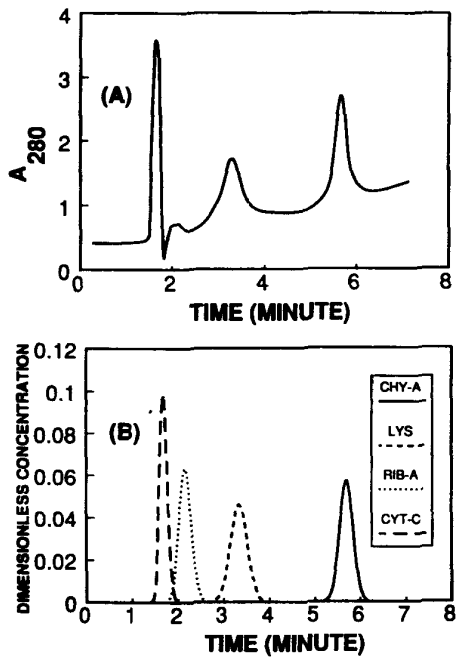

Fig. 29. Chromatograms of 4 min linear gradient elution from 1.7 to 0.6 mol l^{-1} ammonium sulfate. (A) experimental, (B) theoretical through the detailed model; column length: 8 cm; v = 0.138 cm s^{-1}

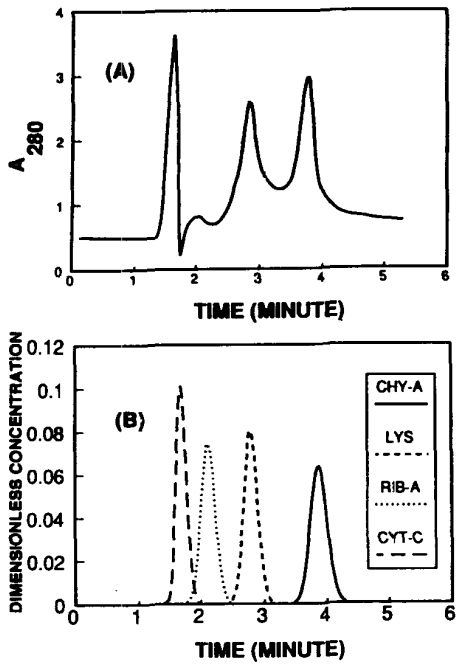

Fig. 30. Chromatograms of 1 min linear gradient elution from 1.7 to 0.6 mol l^{-1} ammonium sulfate. (A) experimental, (B) theoretical through the detailed model; column length: 8 cm; v = 0.138 cm s^{-1}

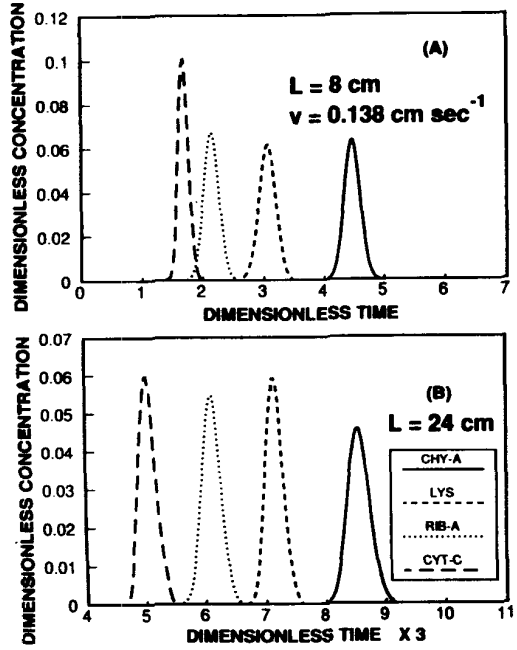

Fig. 31. Comparison of chromatograms of 2 min linear gradient elution from 1.7 to 0.6 mol l^{-1} ammonium sulfate at various column lengths calculated through the detailed model. (A) 8 cm, (B) 24 cm; v = 0.138 cm s^{-1}

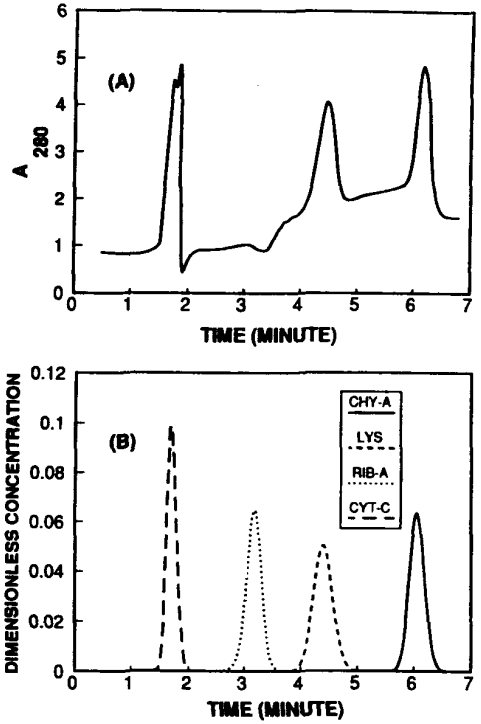

Fig. 32. Chromatograms of multi-stepwise gradient elution of 1 min 2 mol l^{-1}, 2 min 1.3 mol l^{-1}, then 0.6 mol l^{-1} ammonium sulfate sequentially. (A) experimental, (B) theoretical through the detailed model; column length: 8 cm; v = 0.138 cm s^{-1}

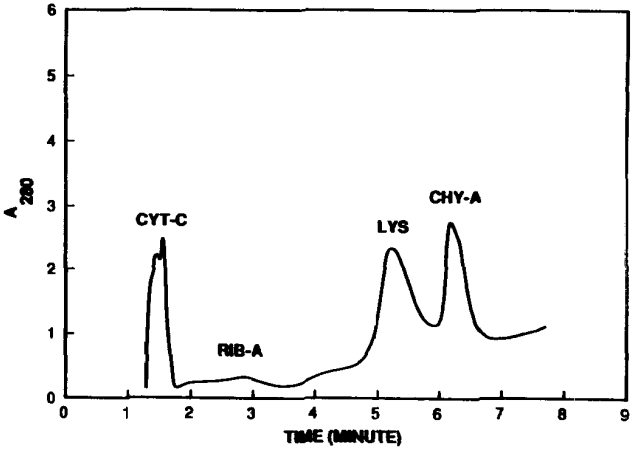

Fig. 33. Chromatogram of multi-stepwise gradient elution of 1.5 min 2 mol l^{-1}, 1.5 min 1.4 mol l^{-1}, then 0.6 mol l^{-1} ammonium sulfate sequentially on a column of Zorbax Bio-series WCX-300 (80 × 6.2 mm) at pH 6 and the flowrate of 1 ml min^{-1}

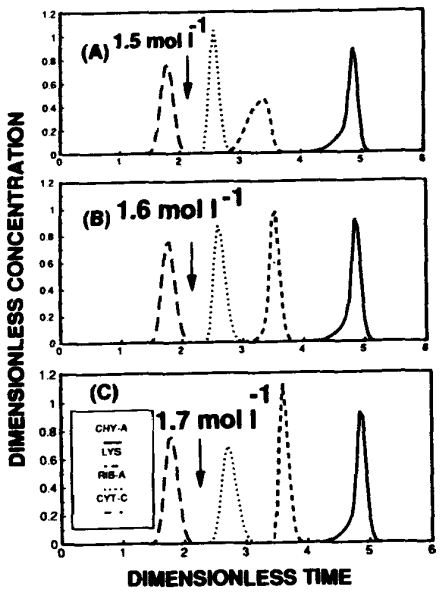

Fig. 34. Chromatograms of multi-stepwise gradient elution of 0.5 min 2 mol l^{-1}, 1.1 min 1.6 mol l^{-1}, 1.4 min 1.1 mol l^{-1}, then 0.5 mol l^{-1} ammonium sulfate sequentially using the gradient elution instrumentation of Scott considering the fluctuation of the second-step eluent concentration through the detailed model; column length: 8 cm; v = 0.138 cm s^{-1}. (A) minus the maximal fluctuation, 0.1 mol l^{-1}, (B) normal, (C) plus the maximal fluctuation

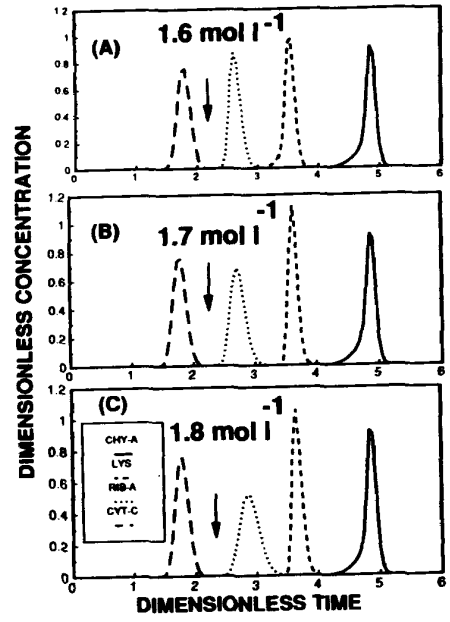

Fig. 35. Chromatograms of multi-stepwise gradient elution of 0.5 min 2 mol l^{-1}, 1.1 min 1.7 mol l^{-1}, 1.4 min 1.1 mol l^{-1}, then 0.5 mol l^{-1} ammonium sulfate sequentially using the gradient elution instrumentation of Scott considering the fluctuation of the second-step eluent concentration through the detailed model; column length: 8 cm; v = 0.138 cm s^{-1}. (A) minus the maximal fluctuation, 0.1 mol l^{-1}, (B) normal, (C) plus the maximal fluctuation

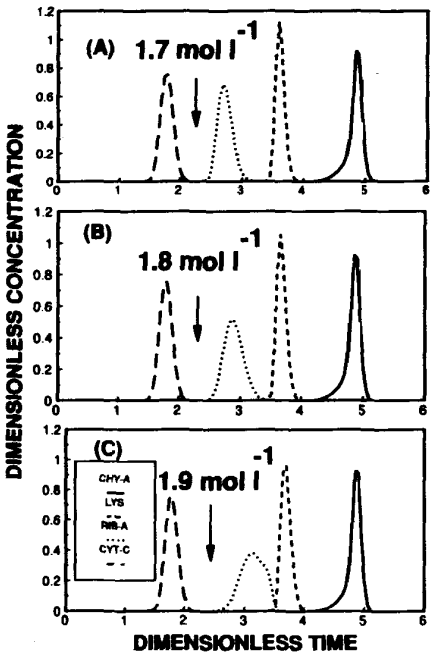

Fig. 36. Chromatograms of multi-stepwise gradient elution of 0.5 min 2 mol l^{-1}, 1.1 min 1.8 mol l^{-1}, 1.4 min 1.1 mol l^{-1}, then 0.5 mol l^{-1} ammonium sulfate sequentially using the gradient elution instrumentation of Scott considering the fluctuation of the second-step eluent concentration through the detailed model; column length: 8 cm; v = 0.138 cm s^{-1}. (A) minus the maximal fluctuation, 0.1 mol l^{-1}, (B) normal, (C) plus the maximal fluctuation

a practical strategy for optimization has been developed using this detailed model, as illustrated in Fig. 37.

After the cation exchange column, the pH value of the mobile phase and the hydrophobic interaction range of the eluent concentration have been chosen, the final eluent concentration of the linear gradient can be determined from the eluent concentration at which the weakest eluate has the minimum b. Then the shortest acceptable gradient period (see Fig. 38) is chosen as the first guess to calculate the ideal retention time of eluates at various initial eluent concentrations of the linear gradient (see Fig. 39) through the concentration wave equation [32]:

$$(dz d\tau^{-1})_i = \{1 + [(1 - \varepsilon_b)\varepsilon_p \varepsilon_b^{-1}] + [(1 - \varepsilon_b)(1 - \varepsilon_p) f'(C_{bi}) \varepsilon_b^{-1}]\}^{-1} \quad (6)$$

where $f'(C_{bi}) = d[a_i C_{bi}(1 + \sum b_j C_{bj})^{-1}] d(C_{bi})^{-1}$, C_b is the eluate concentration, a is a constant in the Langmuir adsorption equation, z is the dimensionless axial coordinate, τ is the dimensionless time, ε_b is the bed void fraction, and ε_p is the particle porosity. Then, the ideal distances of adjacent eluate peaks can be obtained (see Fig. 40). A good separation needs the peak distances to be larger than the dilution ratio of the feed impulse by the pore liquid (see Fig. 41), as $(1 - \varepsilon_b)\varepsilon_p \varepsilon_b^{-1} + \tau_{imp}$.

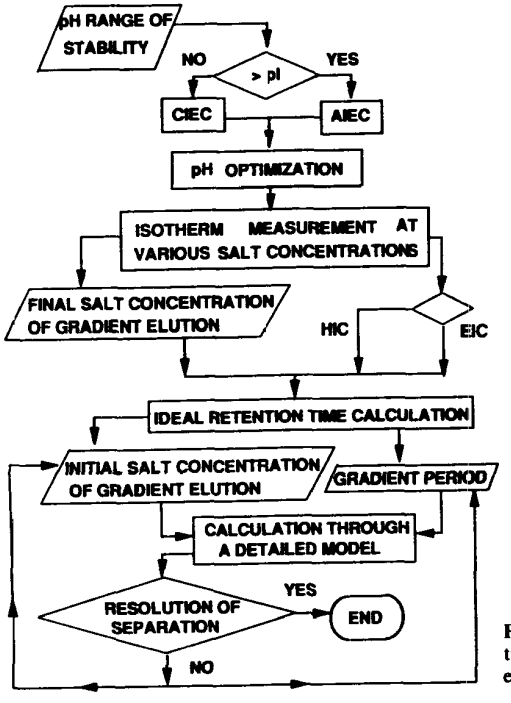

Fig. 37. Flow-sheet illustration of optimization strategy of linear gradient elution chromatography

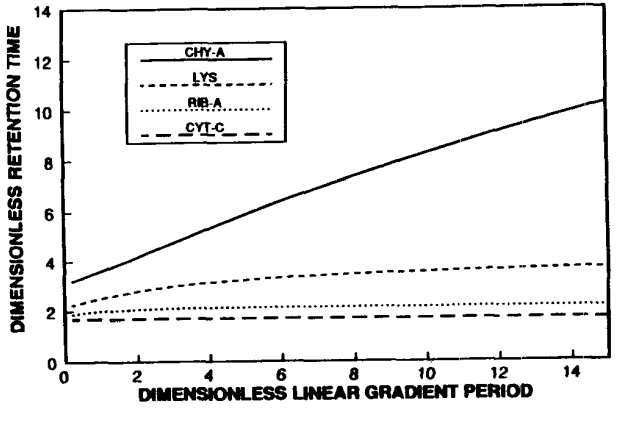

Fig. 38. Retention time vs gradient period of linear gradient elution chromatography calculated through the ideal model

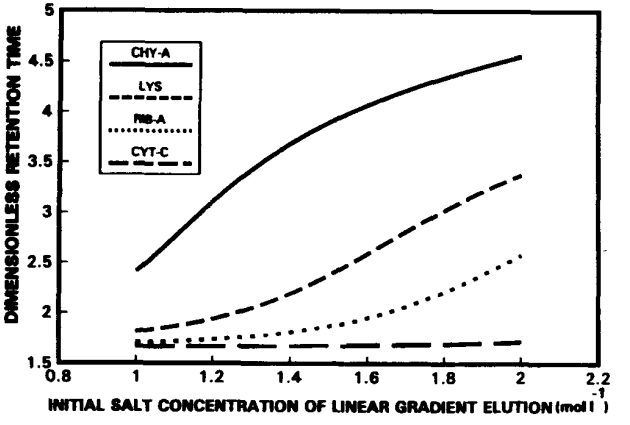

Fig. 39. Retention time vs initial salt concentration of linear gradient elution chromatography calculated through the ideal model

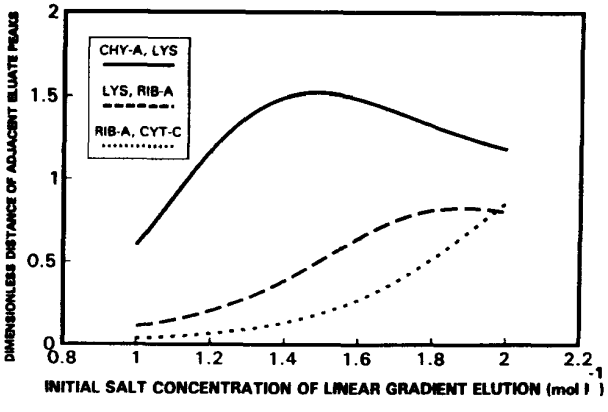

Fig. 40. Distance of adjacent peaks vs initial salt concentration of linear gradient elution chromatography calculated through the ideal model

A first guess for the initial eluent concentration is then chosen, so that the ideal peak distances are larger than the dilution ratio and the strongest eluate has the shortest ideal retention time. The second and the third guesses of the initial eluent concentration will be the first one plus and minus a selected small value, respectively. If the separation result with the second guess is better than with the first guess from the calculation through the detailed model, then the fourth guess will be the second guess plus that certain value, and vice versa. The iteration goes on until the separation result satisfies the criteria of separation resolution. After the optimal initial eluent concentration is determined through

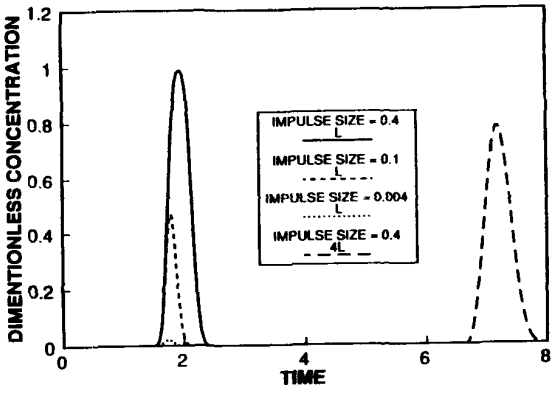

Fig. 41. Dilution of feed impulse by pore liquid of porous chromatographic material

the detailed model, the optimal gradient period also can be determined through the same iteration approach as for the optimal initial eluent concentration using the detailed model.

5.1 Eluent Concentrations

In this case, 1.7 M and 0.6 M ammonium sulfate are the optimal initial and final eluent concentrations, respectively, as shown in Fig. 24. The separation performance according to the optimal eluent concentrations is compared with that of 1.6 M as the initial eluent concentration and 0.4 M as the final eluent concentration of a 2 min linear gradient, shown in Fig. 25.

5.2 Gradient Period

A shorter gradient period of a linear gradient, such as 1 min, can save operation time but lowers the separation performance, as shown in Fig. 28. A longer gradient period, such as 4 or 10 min, can improve the separation performance, but is not time effective, and the bands are broader than in a shorter gradient period, as shown in Figs. 29 and 30. An optimal gradient period, 2 min in this case, can be determined, as shown in Fig. 24.

5.3 Flowrate

For the same elution volume of the eluent solution, the flowrate is inversely proportional to the gradient period. Therefore, increasing flowrate will reduce

the separation performance, as shown in Figs. 24, 26 and 27, although it can save operation time. Increasing flowrate will also result in a high pressure drop within the gradient system. There is usually a pressure limit for most chromatographic devices.

5.4 Column Length

Increasing the column length has long been used as a universal method for improving the separation efficiency [72]. This practice is based on the increase in the distance between the eluate bands due to an increase in column length. However, increasing column length also often broadens the bands. If the increase of the band distance is larger than the increase of the band widths when the column length is increased, the separation performance will be improved. Otherwise, the separation performance can be reduced, as illustrated in Fig. 42 [55].

Longitudinal dispersion, slow film mass transfer, intraparticle diffusion, and adsorption and desorption kinetics, can broaden band profiles [12, 13, 32], and the width of the broadened part of the band is proportional to the time of passage through the column, which is called proportional-pattern behavior [32, 73]. The nonlinear response of the stationary phase at the trailing edge of the band can also broaden it [32]. Thus, the band can be broadened by the increase of the column length, because the time of passage through the column is increased with the column length based on the proportional-pattern behavior.

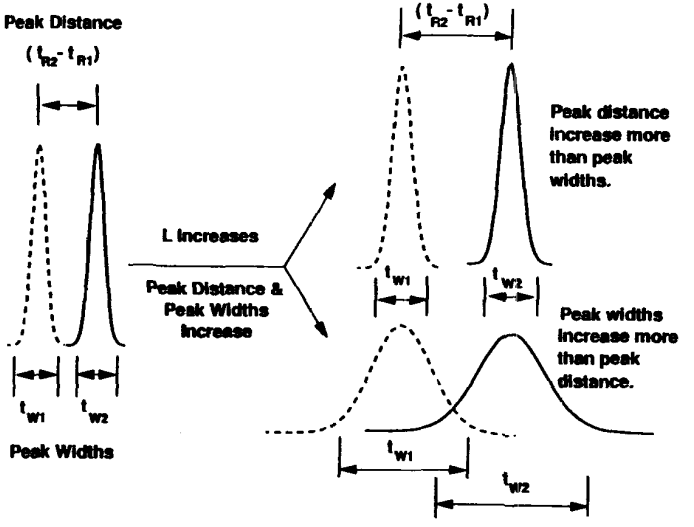

Fig. 42. Illustration of the column length effect on the separation performance

On the other hand, the nonlinear response of the stationary phase on the band front is to make it steeper, the so-called self-sharpening effect, and the width of the band front tends towards a constant value as the band moves through the column, called the constant-pattern behavior [32]. Apparently, the constant-pattern behavior improves and the proportional-pattern behavior damages the separation performance. The conflict between the constant-pattern and the proportional-pattern behaviors can result in a mixed outcome of chromatographic separations, instead of other solely constant-pattern behavior or solely proportional-pattern behavior. Thus, increasing column length is expected to improve or damage the separation performance according to constant-pattern or proportional-pattern behavior, respectively. Then, an optimal column length may exist in a system exhibiting both behaviors, as shown in Fig. 43 [55].

The plate theory indicates that the plate number or the separation efficiency is proportional to the column length [27, 74]. In displacement chromatography, Golshan-Shirazi et al. [75], showed that if the sample is smaller than the optimum loading factor, the isotachic train will be formed before the end of the column and increasing the column length will result in no change in the band profiles, which is consistent with constant-pattern behavior. However, the plate theory is limited to symmetric Gaussian bands and linear chromatography. For asymmetric bands, an optimal column length may exist [55].

Furthermore, the dilution of the injection band by the pore liquid also can broaden the band, as shown in Fig. 41 [55]. However, this phenomenon has long been overlooked. A longer column contains more pore liquid, which also can make the injection band more diluted and broader.

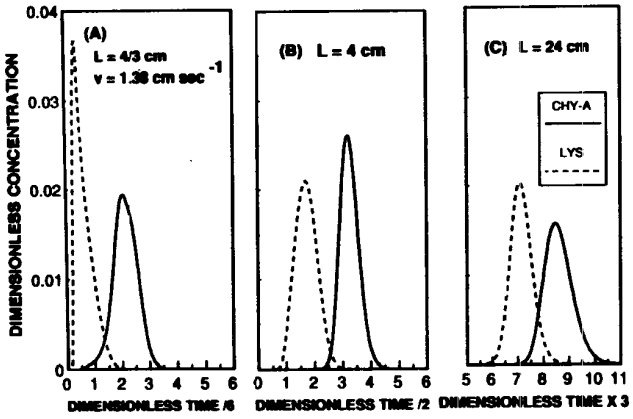

Fig. 43. Comparison of chromatograms of 2 min linear gradient elution from 1.7 to 0.6 mol l^{-1} ammonium sulfate at various column lengths calculated through the detailed model. (A) 4×3^{-1} cm, (B) 4 cm, (C) 24 cm; v = 1.38 cm s^{-1}

5.5 *Gradient Shape*

In comparing linear gradients with stepwise gradients, there is no unique answer to which is better. The ratio of the maximal loading capacity to the operation period can be a standard for the separation performance. However, the stepwise gradient is more cost effective due to its smaller instrument requirements. But, to separate relatively close eluates, the linear gradient usually can achieve better separation relative to the stepwise gradient due to the continual increase of the elution strength throughout the gradient period. Likewise, a similar comparison can be made between linear gradient and isocratic runs. On the other hand, to separate dissimilar eluates, a stepwise gradient could be economical and efficient enough. Furthermore, although nonlinear gradients and segmented linear gradients have the advantage of higher separation efficiency they also have the disadvantage of inconvenient complexity.

5.6 *Process Tolerance to the Fluctuation of Input Parameters*

In industrial operations of chromatographic processes, it is not easy to control the input conditions as precisely as in the laboratory. The particle size of the column material may vary from batch to batch. Pure or reagent grade reagents may not be used in large-scale production. The column capacity may degrade over time [76]. Lot-to-lot consistencies may not be good. Some of the input parameters are uncontrollable such as the concentrations of the bioconversion-generated feeds. Variation of bioconversion potency by 10%–30% among batches is not unusual. The concentrations of some bioconversion-generated trace compounds can vary by hundreds of percentage points. A good separation process must consider not only the separation efficiency but also the process tolerance to the fluctuation of input conditions.

Sometimes, the process tolerance to the fluctuation of input conditions is contradictory to separation efficiency. From the stoichiometric model of reversed phase chromatography, log(k') (k' denotes the capacity factor) is proportional to log(Cm) (Cm denotes the eluent concentration) with a proportional coefficient Z' [58]. The Z' values of proteins can be in the order of hundreds. This implies that a 1% deviation of eluent concentration can result in the change of retention time of the eluates up to 1000%. Therefore, this process has a very good separation efficiency due to the large Z' value, but the process stability has a very poor tolerance to fluctuation of Cm.

The optimization strategy has been developed by considering both the separation efficiency and the process tolerance to the fluctuation of input conditions, as shown in Fig. 44 [55]. A case in point is the fluctuation of the eluent and the eluate concentrations in stepwise gradient elution chromatography, as illustrated in Figs. 34–36. The worst or largest fluctuation of the input parameters must be defined first, 0.1 M for the second-step eluent concentration in this case; then the optimization strategy can be developed to ensure the

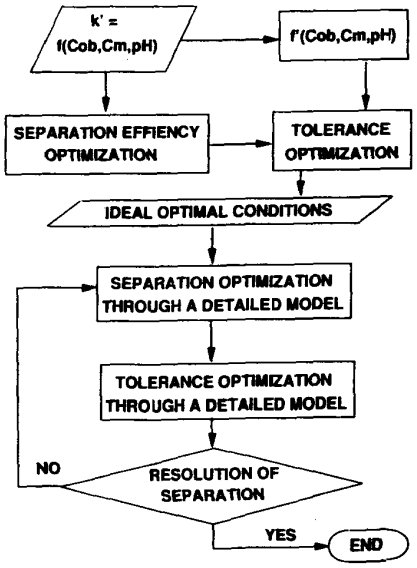

Fig. 44. Flow-sheet illustration of optimization strategy of separation efficiency and tolerance to the fluctuation of input parameters

separation performance under the worst operation conditions. The optimal eluent concentration of the second step in this is 1.6 M, as shown in Fig. 34. However, this optimal eluent concentrations has been adjusted to 1.7 M after considering the process tolerance to the fluctuation of the input parameters, as shown in Fig. 35.

Acknowledgement. This article is prepared with the grant support (EET-8613167A2) from the National Science Foundation.

6 References

1. Jandera P, Churacek J (1985) Gradient elution in column liquid chromatography. Elsevier, Amsterdam
2. Liteau C, Gocan S (1974) Gradient liquid chromatography. John Wiley, New York
3. Schoenmakers PJ (1986) Optimization of chromatographic selectivity. Elsevier, Amsterdam
4. Snyder LR (1980) Gradient elution. In: Horvath C (ed) High-performance liquid chromatography: Advances and prospectives, vol 1. Academic, New York
5. Verzele M, Daweale C, van Dijck J, van Haver D (1982) J Chromatogr 249: 231
6. Knox JH, Pyper HM (1986) J Chromatogr 215: 295
7. Helfferich FG (1962) Ion exchange. McGraw-Hill, New York
8. Frenz J, Cs. Horvath Cs (1985) AIChE J 31: 400
9. Helfferich FG (1986) J Chromatogr 373: 45–60
10. Rhee H-K, Aris R, Amundson NR (1970) Philosophical Transactions Royal Society London 1182: 419

11. Snyder LR (1968) Principles of adsorption chromatography. Marcel Dekker, New York
12. Chase HA (1984) C.E.S. 39: 1099
13. Muller AJ, Carr P (1984) J Chromatogr 294: 235
14. Guiochon G, Ghodbane S, Golshan-Shirazi S, Huang J-X, Katti A, Lin B-C, Ma Z (1989) Talanta. 36: 19
15. Arnold FH, Blanch HW (1986) J Chromatogr 355: 13
16. Arve BH, Liapis AI (1987) AIChE J 33: 179
17. Biyani P, Goochee CF (1988) AIChE J 34: 1747
18. Cen PL, Yang RT (1986) AIChE J 32: 1635
19. Huang CC, Fair JR (1984) AIChE J 34: 1861
20. Seshadri S, Deming SN (1984) Anal Chem 56: 1567
21. Tsou H-S, Graham EE (1985) AIChE J 31: 1959
22. Van Vuuren DS, Stander CM, Glasser D (1984) AIChE J 30: 593
23. Carta G (1988) C.E.S. 43: 2877
24. Furusaki, Haruguchi E, Nozawa T (1987) Bioprocess Engineering 2: 45
25. Horvath Cs, Lin H-J (1976) J Chromatogr 126: 401
26. Horvath Cs, Lin H-J (1978) J Chromatogr 149: 43
27. Snyder LR, Kirkland JJ (1979) Introduction to modern liquid chromatography. Wiley, New York
28. Guiochon G, Golshan-Shirazi S, Jaulmes A (1988) Anal Chem 60: 1865
29. Klein G (1985) AIChE Symposium Series, 242: 28
30. Gu T, Tsao GT, Tsai G-J, Ladisch MR (1990) AIChE J 36: 1156
31. Ruthven DM (1984) Principles of adsorption and adsorption processes. John Wiley, New York
32. Sherwood TK, Pigford RL, Wilke RW (1975) Mass transfer. McGraw-Hill, New York
33. Tokieda T, Tokuda T, Ishida M (1985) Anal Sci 1: 395
34. Jandera P, Churacek J, Colin H (1981) J Chromatogr 214: 35
35. Klotz IM (1946) Archives Biochem 9: 109
36. Mazsaroff I, Varady L, Mouchawar GA, Regnier FE (1990) J Chromatogr 499: 63
37. Melander WR, El Rassi Z, Horvath Cs (1989) J Chromatogr 469: 3
38. Srinivasan R, Ruckenstein E (1980) Separation purification methods 9: 267
39. Melander WR, Horvath Cs (1977) Archives Biochem Biophys 183: 200
40. Roettger BF, Myers JA, Ladisch MR, Regnier FE (1989) Biotechnol Progress 5: 79
41. Yamamoto S, Nomura M, Sano Y (1987) AIChE J 33: 1426
42. Antia FD, Horvath Cs (1989) J Chromatogr 484: 1
43. Ghrist BFD, Snyder LR (1988) J Chromatogr 459: 25
44. Dolan JW (1988) LC-GC 6: 572
45. Weinberger R, Coniglione V (1984) LC 2: 10
46. Berridge JC (1985) Techniques for the automated optimization of HPLC separations. John Wiley, New York
47. Huber JFK (1978) Instrumentation for high-performance liquid chromatography. Elsevier, Amsterdam
48. MacDonald JC (1986) HPLC: Instrumentation and applications. International Scientific Communications, Fairfield, Connecticut
49. Billiet HA, Keehnen PD, de Galan L (1979) J Chromatogr 185: 515
50. Erni, Frei RW (1978) Res Dev 149: 56
51. Martin M, Guiochon G (1978) In: Huber JFK (ed) Instrumentation for high-performance liquid chromatography, Chapter 3. Elsevier, Amsterdam
52. Pao RHF (1961) Fluid mechanics. John Wiley, New York
53. Scott RP (197) J Chromatogr Sci 9: 385
54. Bio-Rad Laboratories Bio-Rad Model 385 Gradient Former Instruction Manual. Richmond, California
55. Truei YH (1991) PhD Dissertation. Purdue University, West Lafayette, Indiana
56. Skidmore GL, Hormann BJ, Chase HA (1990) J Chromatogr 498: 113
57. Heinitz ML, Kennedy L, Kopaciewicz W, Regnier FE (1988) J Chromatogr 443: 173
58. Geng X, Regnier FE (1984) J Chromatogr 296: 15
59. Kopaciewicz W, Regnier FE (1983) Anal Chem 133: 251
60. Pitt WW Jr (1976) J Chromatogr Sci 14: 396
61. Aguilar MI, Hodder AN, Hearn TW (1985) J Chromatogr 327: 115
62. Hearn MTW, Grego B (1983) J Chromatogr 255: 125
63. Mazsaroff I, Cook S, Regnier FE (1988) J Chromatogr 443: 119

64. Jessissen HP (1976) Hoppe Seler's Z Physiol Chem 357: 1727
65. Afeyan NB, Gordon NF, Mazsaroff J, Varady L, Fulton SP, Yang YB, Regnier FE (1985) J Chromatogr 519: 1
66. Yau WW, Kirkland JJ, Bly DD (1979) Modern size exclusion liquid chromatography. Wiley, New York
67. Chung SF, aWen CY (1968) AIChE J 14: 857
68. Wakao N, Oshima T, Yagi S (1958) Kagaku Kagaku 22: 780
69. Cantor and Schimmel, 1980
70. Cooper AR, Barrall II EM (1973) J Applied Polymer Sci 17: 1253
71. Regnier FE, Mazsaroff I (1987) Biotechnol Progress 3: 22
72. Katti AM, Guiochon (1988) J Chromatogr 449: 25
73. Wankat PC, Koo Y-M (1988) AIChE J 34: 1006
74. Gibbs SJ, Lightfoot EN (1986) I&EC Fundam 25: 490
75. Golshan-Shirazi G, Lin B, Guiochon G (1989) Anal Chem 61: 1960
76. Tice PA, Mazsaroff I, Lin NT, Regnier FE (1987) J Chromatogr 410: 43
77. Jandera P, Churacek J (1980) J Chromatogr 192: 19
78. Armstrong DW, Boehm RE (1984) J Chromatogr Sci 22: 378
79. Kennedy L, Kopaciewicz W, Regnier FE (1986) J Chromatogr 359: 73
80. D'Agostino G, O'Hare MJ, Mitchell F, Salomon T, Verllon F (1988) Chromatographia 25: 343
81. Markowski W, Golkiewicz W (1988) Chromatographia 25: 339
82. Martin M (1988) J Liquid Chromatogr 11: 1809
83. Merengo E, Gennaro MC, Baiocchi C, Bertolo P (1988) Chromatographia 25: 413
84. Kang K, McCoy BJ (1989) Biotechnol Bioeng 33: 786